Electronic Supplementary Material (ESI) for New Journal of Chemistry.

Supporting Information

Ultra-small porous WN/W_2C nanoparticles for sustained hydrogen production by polyoxometalate-intercalated pyrolysis strategy

Ying Zhu,[a] Haiyan Zheng,[a] Xinyan Liu,[a] Chunyi Sun,[a*] Man Dong,[a] Xinlong Wang [a*] and Zhongmin Su [a]

[a] *National & Local United Engineering Laboratory for Power Batteries, Key Laboratory of Polyoxometalate Science of Ministry of Education Department of Chemistry, Northeast Normal University Changchun, Jilin 130024, China*

1. Experimental Section

1.1. Material Synthesis

1.1.1. Synthesis of Zn_3Al-NO_3

The Zn_3Al-NO_3 were synthesized through a common hydrothermal method. $Zn(NO_3)_2 \cdot 6H_2O$ (0.03 mol) and $Al(NO_3)_3 \cdot 9H_2O$ (0.01 mol) were dissolved together in 100ml boiling cooled CO_2-removed deionized water to form a salt solution named A. The other 100ml water dissolved 3.2 g (0.08 mol) NaOH to obtain an alkaline solution called B. A and B were poured into a beaker at the same time and stirred vigorously, maintaining PH ≈ 10 at room temperature. The white colloid was then obtained and quickly transferred to a 250 mL Teflon-lined autoclave, heating at 100 °C for 12 h. After the reactor cooled to room temperature naturally, collected white precipitate by centrifugation and washed with boiling cooled water. Subsequently, one half dried at 60 °C for 12 h under vacuum environment for characterization. Dispersed the other half precipitate into 100mL boiling cooled water to form suspension liquid and kept N_2 input for use.

1.1.2. Synthesis of $K_5CoW_{12}O_{40}$

The preparation of $K_5CoW_{12}O_{40}$ was based on the procedure described by Song et al.[1]

1.1.3. Synthesis of Zn_3Al-CoW_{12}

2 mmol of $K_5CoW_{12}O_{40}$ was dissolved in 100 mL boiling cooled to gain polyacid aqueous solution, added it into Zn_3Al-NO_3 slowly then reacted at 60 °C for 5 h. Centrifuged to collect green-yellow precipitate and washed with boiling cooled water for three times. Finally, the obtained product was dried at 60 °C for 12 h in a vacuum.

1.1.4. Synthesis of WN/W_2C@PC-1, WN/W_2C@PC-2, WN/W_2C@PC-3 and W/WN/CCo_2W_4@PC-4

Zn_3Al-CoW_{12} (0.1 g), glucose (2 g), and NH_4Cl (2 g) were added into a 50 mL stainless steel grinding jar with 20 agate balls 5 mm in diameter, then grinded in a ball mill for 1 h at 35 Hz. The mixture was placed in a tube furnace and step-by-step calcination. First, the powder was annealed at 850 °C for 90 min and further heated to 900 °C maintained 30 min with a rate of 5 °C/min under Ar flow. The black solid was finally obtained after naturally cooling to room temperature, then treated it with 3 M HCl under ultrasonic conditions. Subsequently, the product was washed with a large amount of deionized water until the solution was neutral, centrifuged. Finally, the sample was dried at 60 °C overnight for use. WN/W_2C@PC-2, WN/W_2C@PC-3 and W/WN/CCo_2W_4@PC-4 were obtained by the same method as above but change the calcination conditions to 800 °C, 850 °C and 900 °C for 120 min, respectively.

1.1.5. Synthesis of WN@PC-$K_5CoW_{12}O_{40}$, WN@PC-mixture and C-Zn_3Al-NO_3

Zn_3Al-CoW_{12} (0.1 g) used for the synthesis of WN/W_2C@PC-1 was replaced by $K_5CoW_{12}O_{40}$ (0.1g), the mixture of $K_5CoW_{12}O_{40}$ (0.0587g) and Zn_3Al-NO_3 (0.0413g), and Zn_3Al-NO_3 (0.1g), respectively, then treated under the same ball milling and calcination conditions with WN/W_2C@PC-1 to gain WN@PC-$K_5CoW_{12}O_{40}$, WN@PC-mixture and C-Zn_3Al-NO_3.

1.2. Electrode preparation and electrochemical characterization

All the electrochemical measurements of as-synthesized electrocatalysts were performed on an electrochemical station (CHI760E, Shanghai Chenhua Instruments Co, China). An Ag/AgCl (3.5 M KCl solution) electrode and a graphite rod were employed as the reference electrode and counter electrode. For the working electrodes, 5 mg of the catalyst active materials were dispersed in the mixture of ethanol (100 μL), ultrapure water (350 μL) and 50 μL of 5 wt% Nation solution by ultrasonication. All measured potentials were converted to the potential vs. the reversible hydrogen electrode (RHE) according to the Nernst equation below: $E_{RHE} = E_{Ag/AgCl} + 0.059\,pH + 0.197$. For HER measurements, 6 μL of the ink was dropped onto the GC electrode with a diameter of 3 mm and dried naturally at room temperature. As a comparison, commercial Pt/C catalyst (20 wt% platinum in carbon) electrodes were also prepared in the same configuration. The LSV curves were measured deaerated with nitrogen at a scan rate of 5 mV s^{-1} in 0.5 M H_2SO_4 and 1 M KOH aqueous solutions at 25 °C prior to the HER. The catalysts were activated using 20 cyclic voltammetry scans with a scan rate of 100 mV s^{-1} before recording the electrochemical performance. The CV measurements were taken with scan rates of 10, 20, 30, 40, 50, 60, 70, 80, 90 and 100 mV s^{-1}, respectively. EIS spectra were operated with the frequencies in the range of 0.1−100000 Hz at an amplitude of 5 mV.

2. Physical characterization of $Zn_3Al\text{-}CoW_{12}$ and $Zn_3Al\text{-}NO_3$

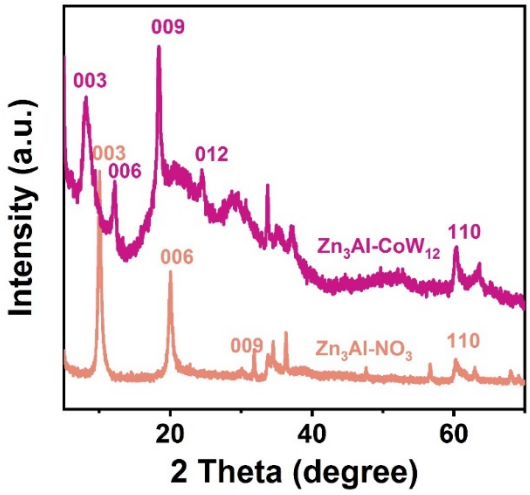

Figure S1. XRD patterns of $Zn_3Al\text{-}CoW_{12}$ and $Zn_3Al\text{-}NO_3$.

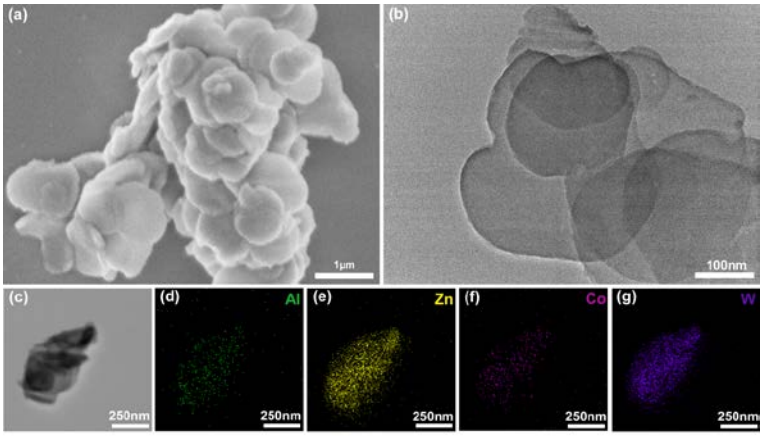

Figure S2. (a) SEM image of Zn_3Al-CoW_{12}. (b) TEM image of Zn_3Al-CoW_{12}. (c-g) EDX elemental mapping of Al, Zn, Co and W in Zn_3Al-CoW_{12}.

3. Physical characterization of electrocatalysts

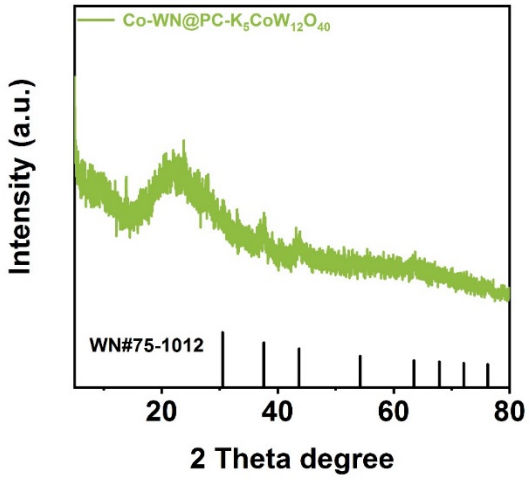

Figure S3. PXRD patterns of WN@PC-$K_5CoW_{12}O_{40}$ (obtained by the calcination of $K_5CoW_{12}O_{40}$).

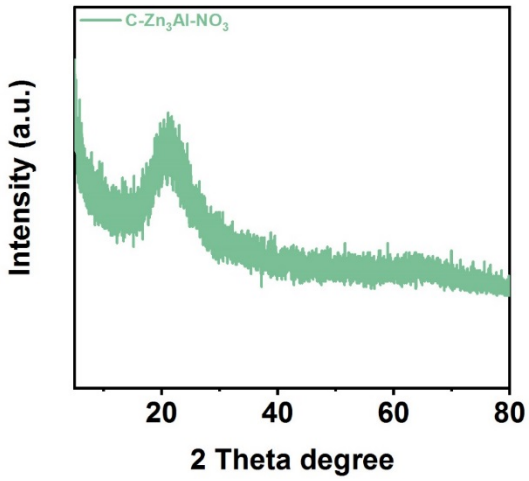

Figure S4. PXRD patterns of C-Zn_3Al-NO_3 (obtained by the calcination of Zn_3Al-NO_3).

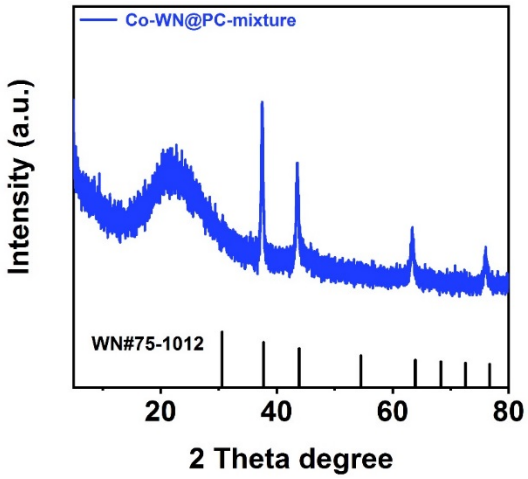

Figure S5. PXRD patterns of WN@PC-mixture (obtain by simple mixture of $Zn_3Al\text{-}NO_3$ and $K_5CoW_{12}O_{40}$).

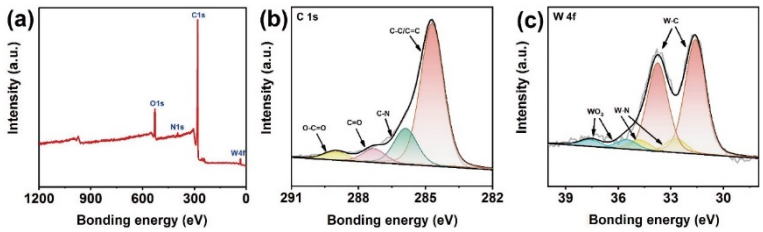

Figure S6. (a) X-ray photoelectron spectra of WN/W_2C@PC-1. (b) The high-resolution C 1s XPS of WN/W_2C@PC-1. (c) The high-resolution W 4f XPS of WN/W_2C@PC-1.

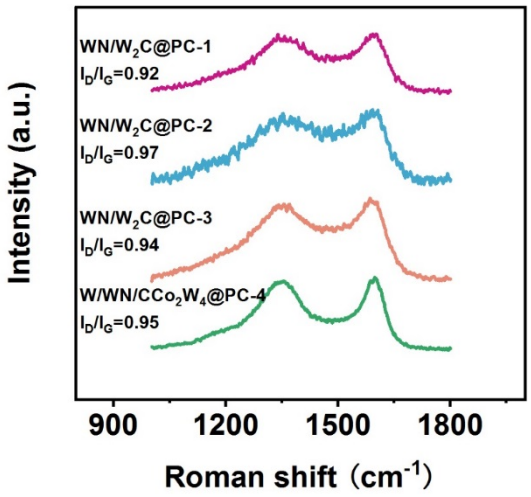

Figure S7. Raman spectra of WN/W_2C@PC-1, WN/W_2C@PC-2, WN/W_2C@PC-3 and W/WN/CCo_2W_4@PC-4.

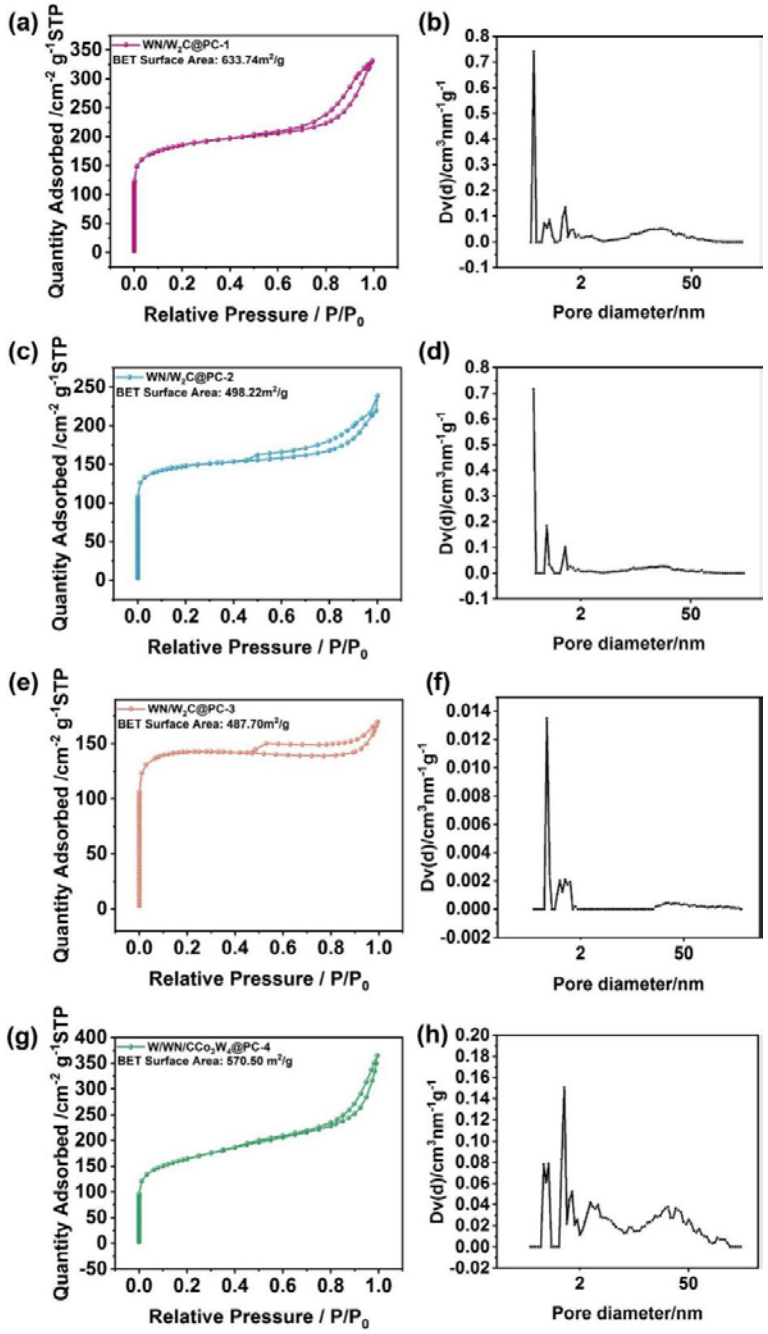

Figure S8. N_2 adsorption-desorption isotherms of (a) WN/W_2C@PC-1, (c) WN/W_2C@PC-2, (e) WN/W_2C@PC-3 and (g) W/WN/CCo_2W_4@PC-4. The pore-size distribution of (b) WN/W_2C@PC-1, (d) WN/W_2C@PC-2, (f) WN/W_2C@PC-3 and (h) W/WN/CCo_2W_4@PC-4.

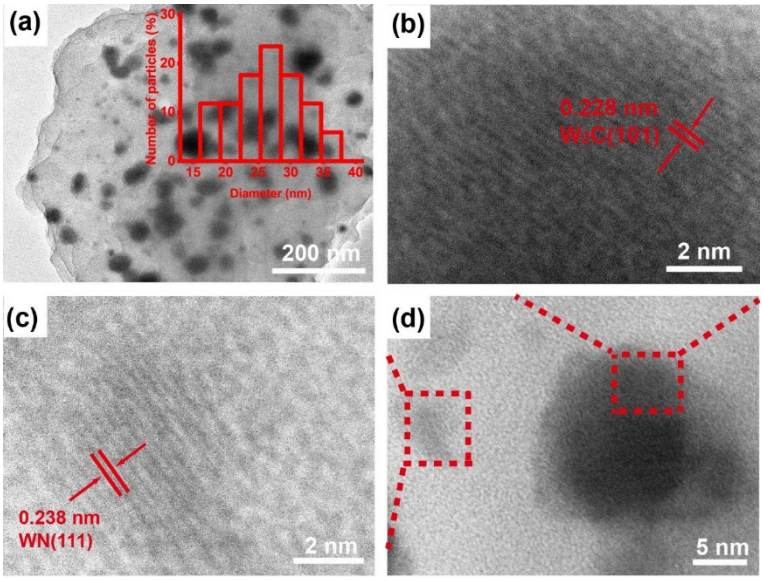

Figure S9. (a) TEM image of WN/W_2C@PC-2 (Inset is the particle size distribution in WN/W_2C@PC-2). (b-d) HRTEM images of WN/W_2C@PC-2.

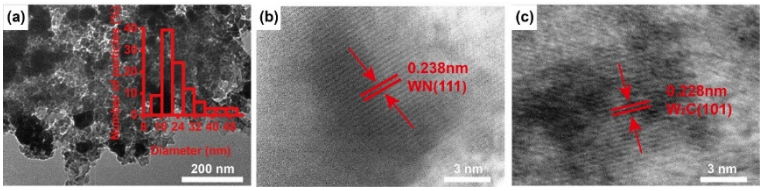

Figure S10. (a) TEM image of WN/W_2C@PC-3 (Inset is the particle size distribution in WN/W_2C@PC-3). (b-c) HRTEM images of WN/W_2C@PC-3.

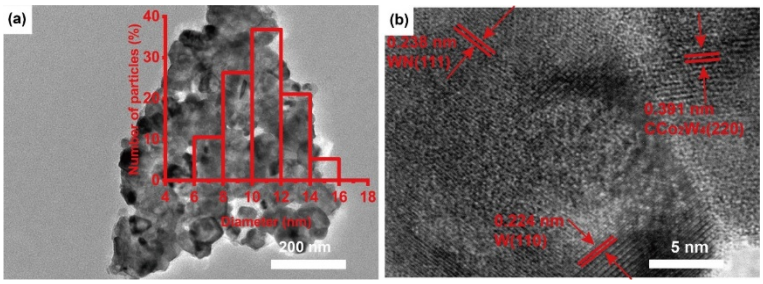

Figure S11. (a) TEM image of W/WN/CCo_2W_4@PC-4 (Inset is the particle size distribution in W/WN/CCo_2W_4@PC-4). (b-d) HRTEM images of W/WN/CCo_2W_4@PC-4.

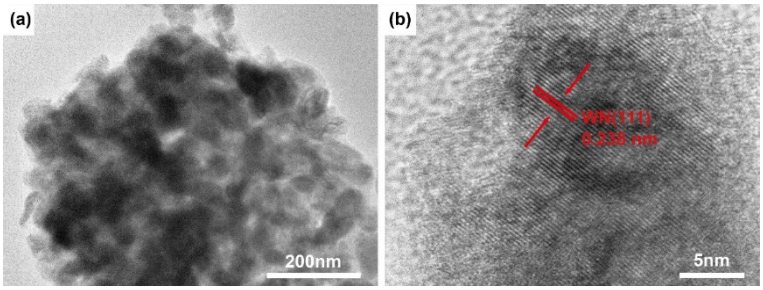

Figure S12. (a) TEM image of WN@PC-mixture. (b) HRTEM image of WN@PC-mixture.

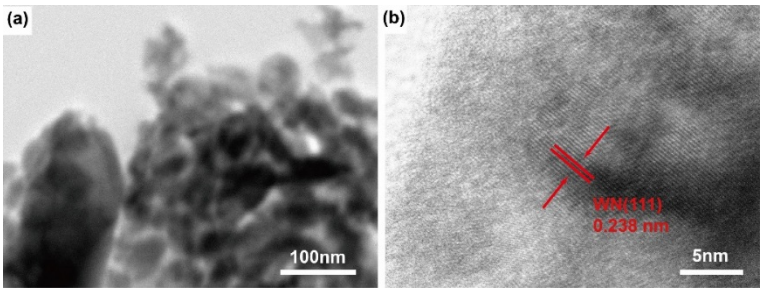

Figure S13. (a) TEM image of WN@PC-$K_5CoW_{12}O_{40}$. (b) HRTEM image of WN@PC- $K_5CoW_{12}O_{40}$.

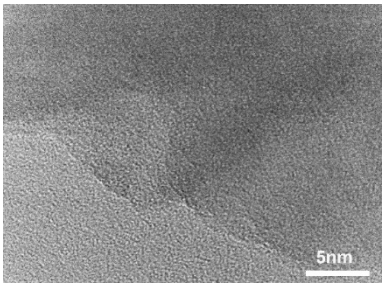

Figure S14. HRTEM image of C-Zn_3Al-NO_3.

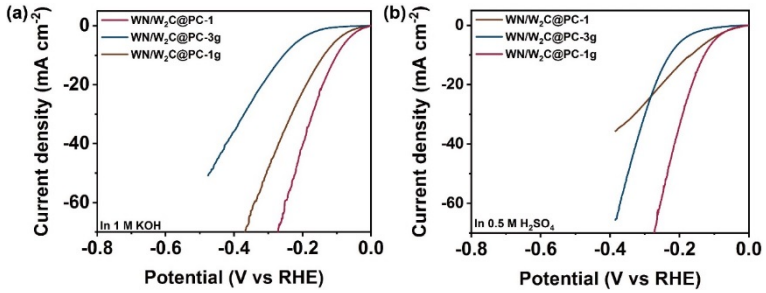

Figure S15. Polarization curves of samples obtained by different amounts of glucose and NH_4Cl in (a) 1.0 M KOH and (b) 0.5 M H_2SO_4.

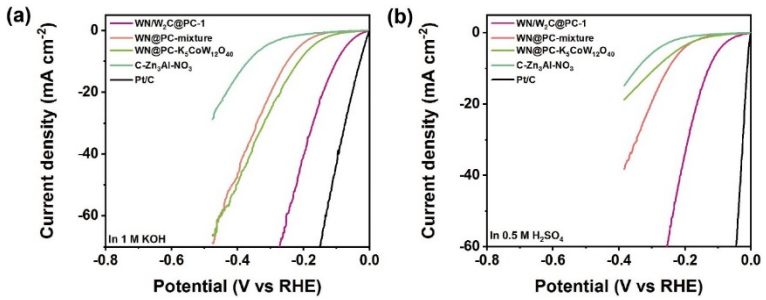

Figure 16. Polarization curves of WN/W_2C@PC-1, WN@PC-mixture, WN@PC-$K_5CoW_{12}O_{40}$ and C-Zn_3Al-NO_3 in (a) 1.0 M KOH and (b) 0.5 M H_2SO_4.

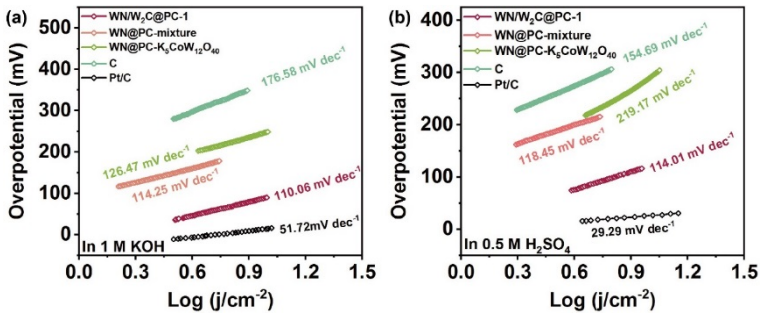

Figure S17. Tafel Slope of WN/W_2C@PC-1, WN@PC-mixture, WN@PC-$K_5CoW_{12}O_{40}$ and C-Zn_3Al-NO_3 in (a) 1.0 M KOH and (b) 0.5 M H_2SO_4.

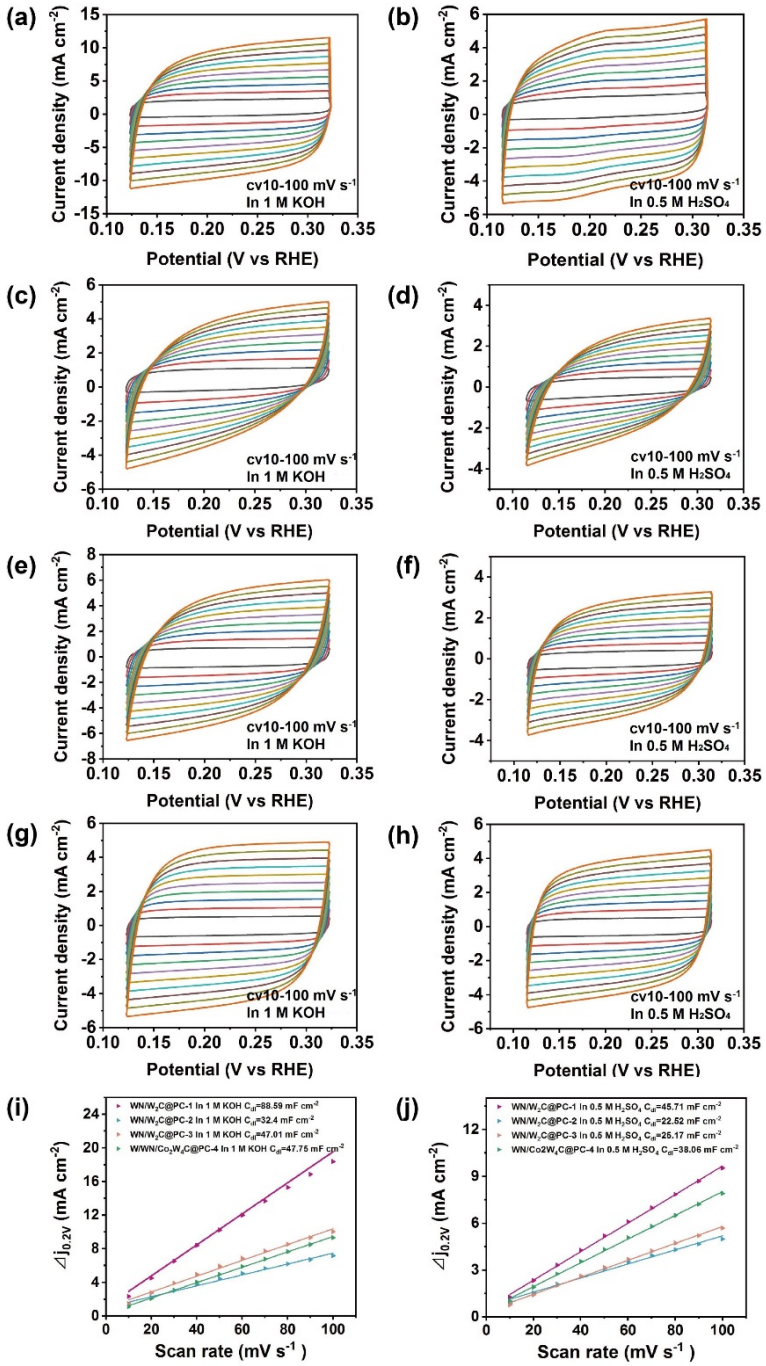

Figure S18 (a-b) Cyclic voltammograms (CVs) of WN/W_2C@PC-1 in 1 M KOH and 0.5 M H_2SO_4. (c-d) Cyclic voltammograms (CVs) of WN/W_2C@PC-2 in 1 M KOH and 0.5 M H_2SO_4. (e-f) Cyclic voltammograms (CVs) of WN/W_2C@PC-3 in 1 M KOH and 0.5 M H_2SO_4. (g-h) Cyclic voltammograms (CVs) of W/WN/CCo_2W_4@PC-4 in 1 M KOH and 0.5 M H_2SO_4. (i-j) Liner fitting of Δj (Δj = j_a - j_c) vs. scan rates at a given overpotential of +0.2V vs. RHE in 1 M KOH and 0.5 M H_2SO_4, respectively. j_a represents the anodic current density and j_c represents the cathodic current density.

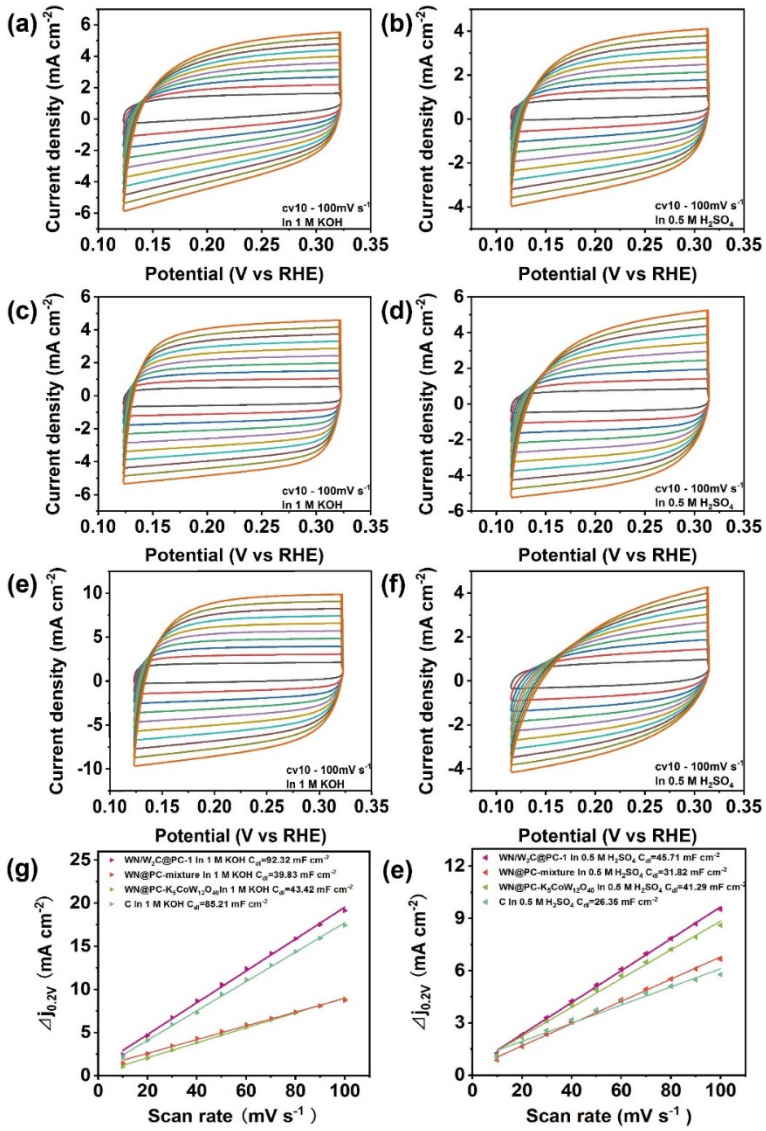

Figure S19. (a-b) Cyclic voltammograms (CVs) of WN@PC-mixture in 1 M KOH and 0.5 M H_2SO_4. (c-d) Cyclic voltammograms (CVs) of WN@PC-$K_5CoW_{12}O_{40}$ in 1 M KOH and 0.5 M H_2SO_4. (e-f) Cyclic voltammograms (CVs) of C-Zn_3Al-NO_3 in 1 M KOH and 0.5 M H_2SO_4. (g-e) Liner fitting of Δj (Δj = j_a - j_c) vs. scan rates at a given overpotential of +0.2V vs. RHE in 1 M KOH and 0.5 M H_2SO_4, respectively. j_a represents the anodic current density and j_c represents the cathodic current density.

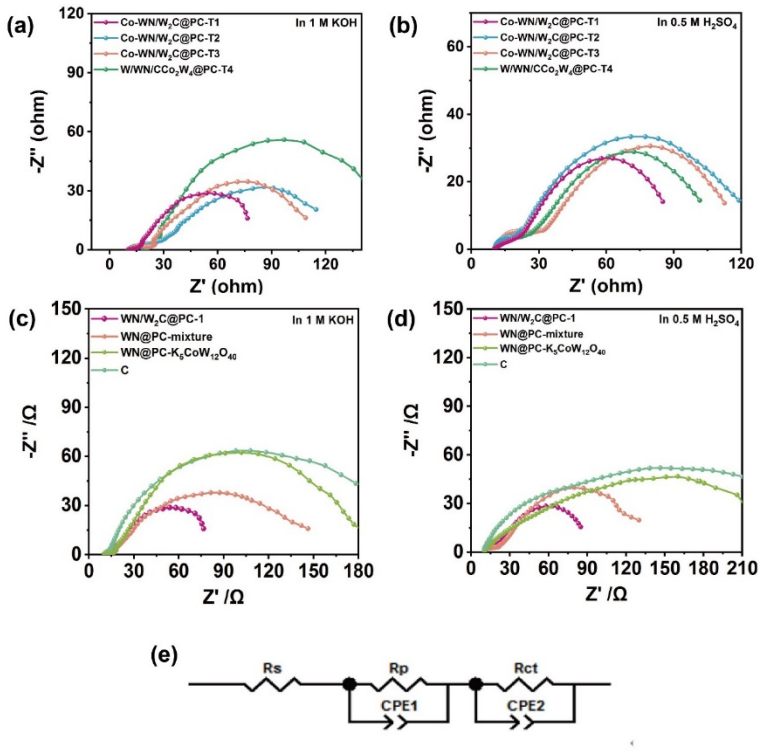

Figure S20. Electrochemical impedance spectra of catalysts obtained by different calcining conditions among 100 kHz to 0.01 Hz in (a) alkaline and (b) acidic media. Electrochemical impedance spectra of single component catalysts obtained among 100 kHz to 0.01 Hz in (a) alkaline and (b) acidic media. (e) The diagram of corresponding equivalent circuit.

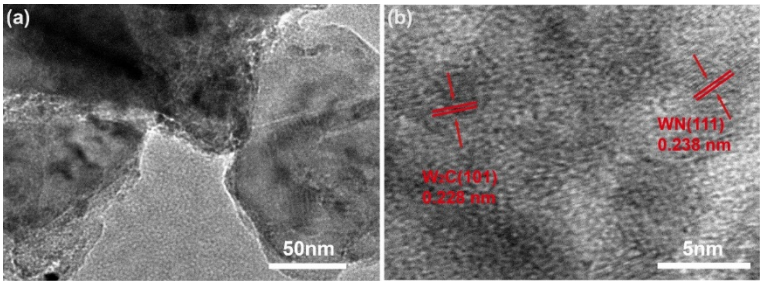

Figure S21. (a) TEM image of WN/W_2C@PC-1 after HER test in 1 M KOH. (b) HRTEM images of WN/W_2C@PC-1 after HER test in 1 M KOH.

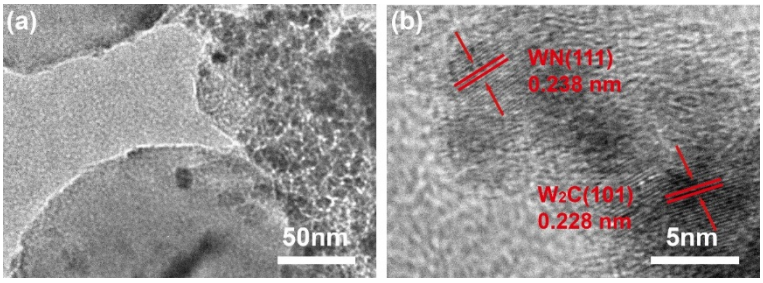

Figure S22. (a) TEM image of WN/W_2C@PC-1 after HER test in 0.5 M H_2SO_4. (b) HRTEM images of WN/W_2C@PC-1 after HER test in 0.5 M H_2SO_4.

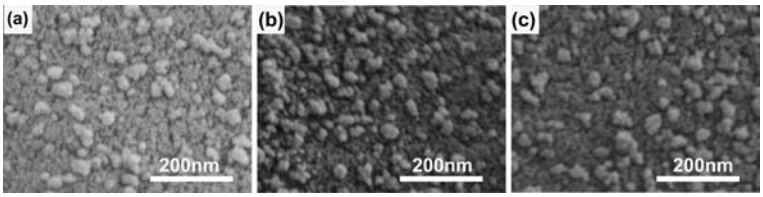

Figure S23. (a) SEM image of WN/W_2C@PC-1 (a) before HER test (b) after HER test in 1 M KOH (c) after HER test in 0.5 M H_2SO_4.

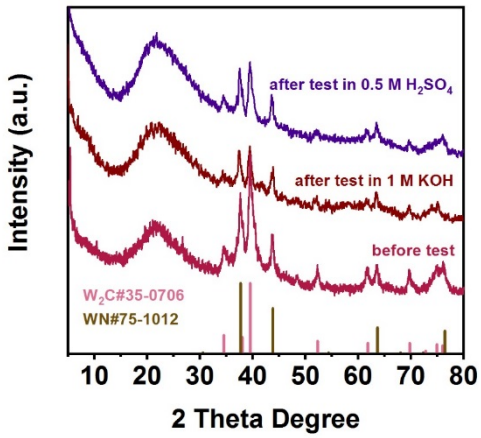

Figure S24. XRD patterns of WN/W_2C@PC-1 after HER test in 0.5 M H_2SO_4 and 1 M KOH.

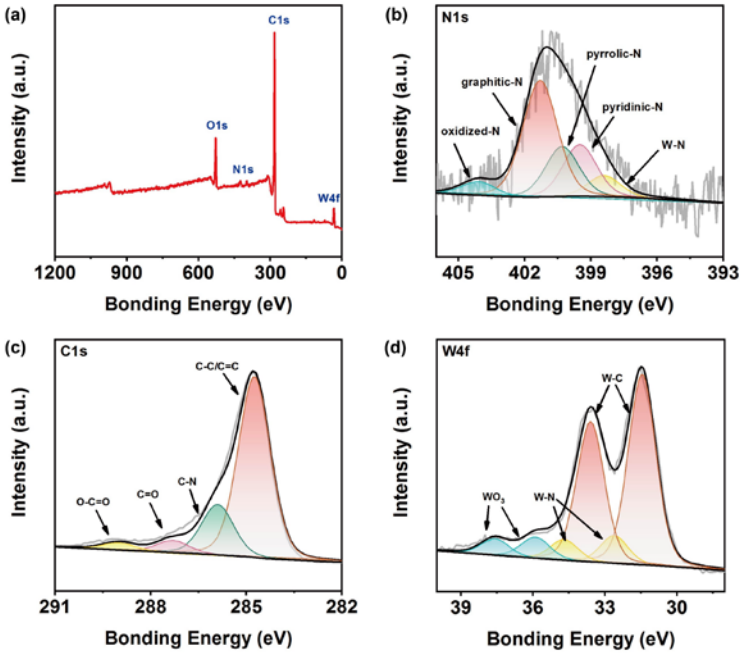

Figure S25. (a) X-ray photoelectron spectra of WN/W_2C@PC-1 after HER test in 1 M KOH. (b) The high-resolution N 1s XPS of WN/W_2C@PC-1 after HER test in 1 M KOH. (c) The high-resolution C 1s XPS of WN/W_2C@PC-1 after HER test in 1 M KOH. (d) The high-resolution W 4f XPS of WN/W_2C@PC-1 after HER test in 1 M KOH.

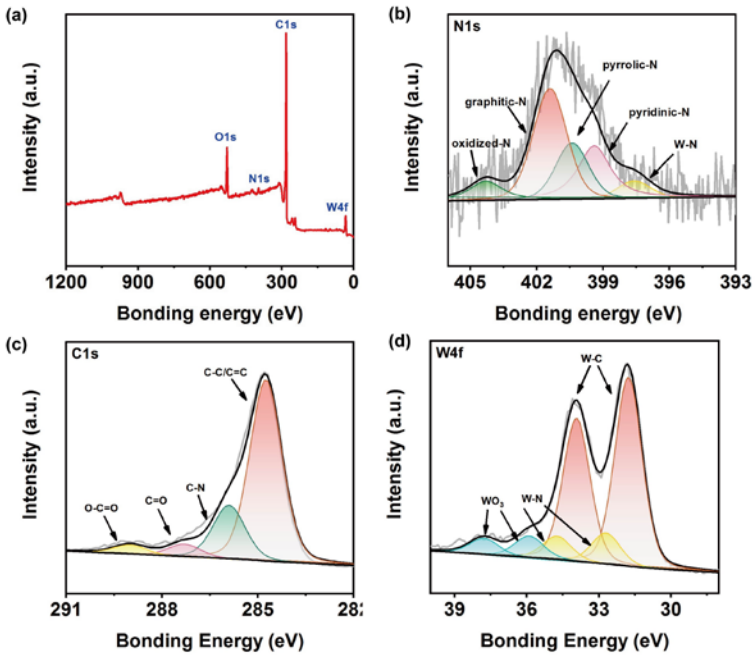

Figure S26. (a) X-ray photoelectron spectra of WN/W_2C@PC-1 after HER test in 0.5 M H_2SO_4. (b) The high-resolution N 1s XPS of WN/W_2C@PC-1 after HER test in 0.5 M H_2SO_4. (c) The high-resolution C 1s XPS of WN/W_2C@PC-1 after HER test in 0.5 M H_2SO_4. (d) The high-resolution W 4f XPS of WN/W_2C@PC-1 after HER test in 0.5 M H_2SO_4.

4. Comparison of electrocatalysts parameters of different non-Pt catalysts

Table S1. Comparison of HER activities in acidic solution for WN/W_2C@PC electrocatalysts.

Catalysts	Current density (j, mA cm^{-2})	η at corresponding j (mV)	Ref.
WN/W_2C@PC	**10**	**121.3**	**This work**
WN NW/CC	10	134	J. Mater. Chem. A 5 (2017) 19072
WC-CNTs	10	145	ACS Nano 9 (2015) 5125–5134
P-W_2C@NC	10	89	J. Mater. Chem. A 5 (2017) 765
W_2C/MWNT	10	123	Nat. Commun. 7 (2016) 13216
W−W_2C/CNT	10	155	ACS Sustainable Chem. Eng. 7 (2019) 10016−10024
$W_2C@WC_{1-x}$/Mo	10	58	J. Mater. Chem. A 8 (2020) 19473
CoP/NCNT-CP	10	165	ACS Sustainable Chem. Eng. 7 (2019) 10044–10051
CoFeNiMo@NCNT	10	209.9	Appl. Catal. B Environ. 280 (2021) 119421
Ni/Mo_6Ni_6C@C	10	122	Chem. Eng. J. 405 (2021) 12696

Table S2. Comparison of HER activities in basic solution for WN /W_2C@PC electrocatalysts.

Catalysts	Current density (j, mA cm^{-2})	η at corresponding j (mV)	Ref.
WN/W_2C@PC	**10**	**91**	**This work**
W_2N/WC	10	148.5	Adv. Mater. 32 (2020) 1905679
WC-CNTs	10	150	ACS Nano 9 (2015) 5125–5134
Mo-WC@NCS	10	179	Nano Energy 74 (2020) 104850
δ-WN/Fe	10	209	J. Mater. Chem. A 6 (2018) 10967
W−W_2C/CNT	10	147	ACS Sustainable Chem. Eng. 7 (2019) 10016−10024
Mo_2C-WC/NCAs	10	126	Chem. Eng. J. 408 (2021) 127270
CoP/NCNT-CP	10	230	ACS Sustainable Chem. Eng. 7 (2019) 10044–10051
$(Fe_{0.75}Co_{0.25})_5C_2$	10	174	Science Bulletin 63 (2018) 1358–1363
Fe_7S_8/FeS_2	10	113	Adv. Funct. Mater. 32 (2022) 2107802

[1] T. Li, L. Jin, W. Zhang, H.N. Miras, Y.F. Song, ChemCatChem 10 (2018) 4699-4706.